Changes in the urinary proteome in a Patient-Derived Xenograft model

Yongtao Liu[1], Youzhu Wang[2], Zhixiang Cao[2] and Youhe Gao[1*]

1. Department of Biochemistry and Molecular Biology, Gene Engineering Drug and Biotechnology Beijing Key Laboratory, Beijing Normal University, Beijing 100875, China
2. Beijing Percans Oncology Co. Ltd, Beijing 102206, China

Abstract

In this report, the urinary proteome from a patient-derived xenograft (PDX) model was compared at the peptide level to study the origins of urinary proteins in tumor-bearing nude mice. Urine was collected from the PDX mice before and after tumor implantation. A total of 515 mouse proteins were identified, of which 8 were differential proteins. Seventy-eight unambiguous human peptides from 42 human proteins were identified in the tumor-bearing group. Compared with the differential urinary proteins from the tumor-bearing immuno-competent rats, the differential proteins in the urine from the PDX model had no host immune response proteins in the very early stage urine in the tumor-bearing immuno-competent rat model.

Keywords: Cancer biomarker; Urinary proteins; PDX model

Correspondence

Youhe Gao, Department of Biochemistry and Molecular Biology, Gene Engineering Drug and Biotechnology Beijing Key Laboratory, Beijing Normal University, Beijing, 100875, China.
Tel: 86 10 5880 4382; Fax: 86 10 6521 2284; E-mail: gaoyouhe@bnu.edu.cn

Funding Information

This work was supported by the National Key Research and Development Program of China (2016YFC1306300); Beijing Natural Science Foundation (7173264,7172076); funds from Beijing Normal University (11100704, 10300-310421102) and pumch-2016-2.27. The funders had no role in study design, data collection and analysis, decision to publish, or preparation of the manuscript.

Introduction

Biomarkers are measurable changes associated with a physiological or pathophysiological process. Blood remains stable and balanced due to the homeostatic mechanisms of the body. In contrast, the urine is where most blood wastes are disposed, and thus, urine exhibits larger change (Gao,2013).

Many reports found candidate biomarkers in the urine in the very early stage of disease. Pulmonary fibrosis-related proteins were detected before the formation of pulmonary fibrosis in the urine of a rat model, and if therapy could begin this timepoint, prednisone, which is ineffective in late stages, could effectively stop fibrosis development (Wu, 2017). In liver fibrosis model, urinary proteins underwent change earlier than aminotransferase and other indicators in the blood, and many of the changed proteins were associated with liver fibrosis, cirrhosis and their formation mechanisms (Zhang,2017). In a multiple sclerosis model, changes in the urine proteome could be seen even before pathological changes occurred. Among the 7 proteins that changed the most, 6 were reported to be associated with multiple sclerosis (Zhao,2017). The urinary proteins changed in a chronic pancreatitis rat model, and some of those differential urinary proteins were reported to be pancreatitis-related (Zhang,2018). Several urinary proteins changed in a chronic obstructive pulmonary disease (COPD) rat model, and some of those candidate markers are COPD-associated (Huang, 2018). Many differential urinary proteins were detected in urine from a bacterial meningitis model, many of which are reported in cerebrospinal fluid and blood as biomarkers of bacterial meningitis (Ni,2017).

The Walker 256 tumor cell line was subcutaneously injected into rats, and the urinary proteome changed significantly even before a tumor mass was palpable in the subcutaneous tumor model. Some of these proteins are reported as tumor markers or are associated with vaccine-related tumors (Wu, 2017). Similarly, C6 glioma cells were injected into rat brains and changes in the urinary proteome were found before detection by magnetic resonance imaging (MRI). Many of these differential urinary proteins were previously reported to be associated with glioma (Ni,2017).

Since differential urinary proteins are present in the very early stages of cancer cell implantation, it is difficult to imagine that such a substantial change in the urine resulted from a small number of tumor cells. We wondered whether it was possible that theses urinary proteome changes resulted from the host response. In this study, we attempted to answer this using a patient-derived xenograft model (PDX model). As typical immunodeficient animals, nude mice have no normal T-cell immunity. Human tumor cells can easily grow into tumors in these mice. If most of the changes came from the implanted human tumors, human proteins should be unambiguously identifiable in the urine. If most of the early changes were from the host defense, some of the immune-related differential proteins in the nude mice would be missing compared to the differential urinary proteins from immuno-competent animals.

Intestinal tumor cells from patients were implanted subcutaneously into nude mice to construct the PDX model. Urine samples from nude mice were collected after tumors had formed. Urinary proteins were digested in-gel and profiled by LC-MS/MS.

Materials and Methods

Tumor acquisition and PDX model establishment

Fresh tumor samples of at least 6 mm × 6 mm × 6 mm (>200mm^3) were obtained in situ or

from metastatic colorectal cancer tissue after surgery. The sampling sites showed highly malignant tissue activity. After collection, the samples were repeatedly rinsed with precooled sterile saline and immediately placed in a precooled specialized preservative solution. The patient's tumor tissues were transported to the laboratory at 4 °C and placed into a plate with RPMI-1640 medium (Gibco, USA). Tumor tissues were cleaned, and connective tissue, blood vessels, adipose tissue, calcification, and necrosis, were removed from the surface. Tumor tissues were selected and cut into 3 to 5-mm^3 tumor blocks. Tumor growth in NOD/SCID inoculated at 4 subcutaneous points was observed daily. When the tumors reached a set volume, the tumor-bearing mice were sacrificed and the tumors dissected. Next, the tumors were cleaned, cut into small pellets of dimensions 3 mm × 3 mm × 3 mm, and inoculated subcutaneously into BALB-/-c-nu mice. Each mouse was inoculated at 1 point. After 23 days, urine was collected when the tumor volume reached 300 mm^3.

Urine collection and sample preparation

Animals were placed in metabolic cages overnight (for 8 h) individually to collect urine samples. During urine collection, mice had free access to water but no food to avoid urine contamination. Urine were stored at -80 °C and then centrifuged at 4 °C and 12,000 ×g for 30 min to remove cell debris. The supernatants were precipitated with three volumes of precooled acetone at -20 °C for 2 h followed by centrifugation at 4 °C and 12,000 ×g for 30 min. The precipitate was then resuspended in lysis buffer (8 mol/L urea, 2 mol/L thiourea, 25 mmol/L DTT and 50 mmol/L Tris)[7]. Protein concentrations were measured using the Bradford assay.

Tryptic digestion

Urine samples from eight mice each from the control and tumor-bearing groups were selected and analyzed by mass spectrometry with in-gel digestion. Eighty micrograms of total protein was added to the preformed gel (Invitrogen, 8-12%, Carlsbad, CA), and the protein was separated by electrophoresis at 200 V ,40 min and dyed with Coomassie blue for subsequent easier to fading. Each gel was cut from the bottom up into 5 parts based on concentration, and each section was cut into 1 to 1.5-mm^3 pellets. The pellets were washed with 25 mmol/L ammonium bicarbonate / acetonitrile (1:1 V/V) until the pellets were discolored. DTT was used at 20 mmol/L and 37 °C for 1 h to denature the disulfide bonds in the protein structure, and 55 mmol/L IAA was add for 30min in dark to alkylate the disulfide binding sites. Next, 5 ng/L trypsin (Trypsin Gold, Promega, Fitchburg, WI, USA) was added to the dried gel pellets and incubated at 37 °C overnight. Peptides were collected with 50 % acetonitrile, lyophilized and stored at -80 °C.

LC-MS/MS analysis

Reconstituted peptides were desalted by C18 zip tip (Millipore, Germany) and dissolved in 0.1% formic acid. The Thermo EASY-nLC 1200 chromatographic system was loaded onto the precolumn and analytical column. Data were collected by the Orbitrap Fusion Lumos mass spectrometry system (Thermo, USA). The liquid chromatography method was as follows: precolumn: 75 μm × 2 cm, nanoViper C18, 2 μm, 100 Å (Thermo Fisher Scientific, USA), analytical column: 50 μm × 15 cm, nanoViper C18, 2 μm, 100 Å injection volume: 2 mL. The flow rate was 250 nL/min. Phase A was 0.1% formic acid/water (Fisher Scientific, Spain); phase B

was 80% acetonitrile (Fisher Chemical, USA)/0.1% formic acid/20% water. The ion source was nano ESI, and MS data were collected by Orbitrap with a resolution of 120,000, ion charge range of 2-7, and 32% HCD. Secondary MS data were collected by Orbitrap with a resolution of 30,000.

Label- free proteome quantification

Proteomic data were searched using the SwissProt *Homo sapiens* and *Mus musculus* databases (updated Sep 2017). Proteome Discoverer 2.1 software was used for processing. The search parameters were set as follows: the MS deviation of the peptide precursor and product ions was 0.05 Da; the ureido methylation was immobilized to cysteine, variable modifications were made to protein N-terminal acetylation and methionine oxidation, and two missing trypsin cleavage sites were allowed. The peptide FDR was less than 1%, and at least 2 specific peptides were identified pre protein.

Bioinformatics analysis

Urine samples information for the nude mice was obtained from online freeware, DAVID Bioinformatics Resources 6.8 (https://david.ncifcrf.gov) for protein molecular functions, cell components, and biological processes.

Results and Discussion

Nude mice weights and tumor situation

The weights of nude mice in the tumor-bearing group increased slightly within days. As the size of the tumors increased, the net weight of the mice declined, but total weight remains the same, at an overall level of approximately 19-23g. The tumors in the tumor-bearing mice had a volume of approximately 300 mm^3 when inoculated into BALB/c-nu mice for 23 days (**Figure 1**).

Figure 1. Nude mice in the tumor-bearing group. Tumor tissue was implanted subcutaneously in the right rear forelimb.

SDS-PAGE analysis for urinary proteins

SDS-PAGE was used to compare urinary protein differences between the tumor-bearing mice and the control group (**Figure 2**). The differences were noted as followed: for the same sample amount, the tumor-bearing mice showed protein expressions of approximately 70 kDa, which was slightly increased, while the protein expression at 14 kDa decreased slightly. In general, no significant band appearance or disappearance was noted. From this SDS-PAGE result, 8 samples

were selected from both the tumor-bearing and control groups, and their gels were extracted. Each

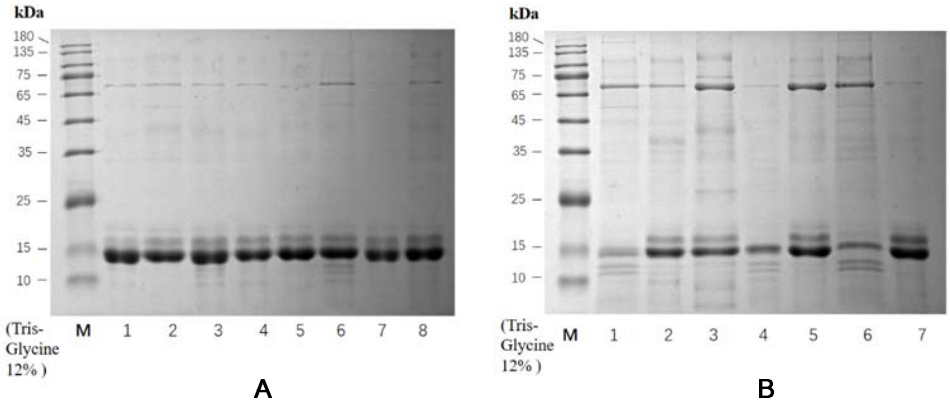

Figure 2. SDS-PAGE analysis of nude mouse urinary proteins. A: control group(n=8); B: tumor-bearing group (n=7).

gel was cut into 5 small samples, for a total 40 samples. After gel digestion, the proteins were broken down into peptides, and samples were analyzed by LC-MS/MS.

Urinary protein profiling from the PDX model

After processing by Protein Discoverer 2.1, the MS data were searched in the *Homo sapiens* and *Mus musculus* databases, to obtain protein names and peptide sequencing information. In total, 515 proteins were detected from the samples included both the control group and the tumor-bearing groups, and for each protein, at least 2 specific peptides were found. Two hundred four human proteins were detected, and after eliminating homologous proteins, 78 human-specific peptides and 42 proteins were obtained.

Unambiguous human proteins

In the PDX model, when tumors were grown to 300 mm^3, 42 unambiguous human proteins were found in the nude mice urine. Each human protein was searched in the human urinary protein database (https://www.urimarker.com/urine/) [9], which contains information on nearly 6,000 normal human urinary proteins. This database online and contains the most comprehensive information on human urinary protein biomarkers. By searching this database, protein abundances for each protein in normal human urine were determined.

Of the 42 human proteins, 21 were reported in normal human urine, of which 16 were high-abundance proteins (concentration greater than 1000 pg/mL), 3 were moderate-abundance proteins (concentration greater than 100 pg/mL), 2 were low-abundance proteins (concentration less than 100 pg/mL), and the other 21 did not appear in normal human urine. **Table 1** shows information on the numbers of total human proteins and specific peptides and their concentrations in normal human urine.

Table 1. Human urinary protein information in tumor-bearing nude mice

Accession	Protein description	Identification	Unique peptide	Concentration in

		counts	counts	human urine (pg/mL)
B4DV14	highly similar to Napsin-A	69 (4/4)	1	not found
A1A508	PRSS3 protein (PRSS3)	44(1/4)	1	not found
D9YZU5	Beta-globin (HBB)	33(1/4)	6	73156.39
P99999	Cytochrome c (CYCS) [*,†]	26(3/4)	4	235.11
A8K7G6	highly similar to *Homo sapiens* regenerating islet-derived 1 alpha	22(1/4)	3	not found
A0A087WXI5	Cadherin-1 (CDH1) [*,†]	17(3/4)	4	61234.54
P48304	Lithostathine-1-beta (REG1B) [†]	14(1/4)	1	not found
A0A0A6YYJ4	Trefoil factor 3 (TFF3) [†]	13(2/4)	4	13032.49
P04083	Annexin A1 (ANXA1) [*,†]	12(1/4)	1	25421.29
P01037	Cystatin-SN (CST1)	11(1/4)	5	3490.18
A0A024RAM2	Glutaredoxin (Thioltransferase) (GLRX) [*]	9(2/4)	1	not found
P01036	Cystatin-S (CST4)	7(1/4)	1	4655.98
A0A1K0GXZ1	Globin C1 (GLNC1)	7(1/4)	2	not found
S6B294	IgG L chain	7(1/4)	1	not found
H9ZYJ2	Thioredoxin (TXN) [*,†]	7(2/4)	2	not found
P36957	Dihydrolipoyllysine (DLST) [*,†]	6(1/4)	1	4061.93
V9HWA9	Epididymis secretory sperm binding protein Li 62p (HEL-S-62p)	6(1/4)	2	not found
Q8TAX7	Mucin-7 (MUC7)	6(1/4)	3	not found
Q6N092	DKFZp686K18196	6(2/4)	3	not found
Q99988	Growth/differentiation factor 15 (GDF15) [*,†]	4(2/4)	2	3499.81
A0A1U9X8X6	CDSN	3(1/4)	1	not found
P04406	Glyceraldehyde-3-phosphate dehydrogenase (GAPDH) [*,†]	3(1/4)	1	20395.34
P31151	Protein S100-A7 (S100A7)	3(2/4)	2	1600.63
Q96DA0	Zymogen granule protein 16 homolog B (ZG16B)	3(1/4)	2	14970.59
Q8N4F0	BPI fold-containing family B member 2 (BPIFB2)	2(1/4)	2	752.72
A9UFC0	Caspase 14 (CASP14)	2(1/4)	2	not found
Q76LA1	CSTB [*,†]	2(1/4)	2	not found
P01040	Cystatin-A (CSTA)	2(1/4)	2	1309.68
Q05DB4	HEBP2	2(1/4)	2	not found
A7Y9J9	Mucin 5AC	2(1/4)	2	not found
Q03403	Trefoil factor 2 (TFF2) [†]	2(1/4)	1	59910.81
Q13867	Bleomycin hydrolase (BLMH) [†]	1(1/4)	1	262.38
Q8TCX0	Delta 2-isopentenyl pyrophosphate	1(1/4)	1	not found

	transferase-like protein			
V9HW80	Epididymis luminal protein 220 (HEL-S-70)	1(1/4)	1	not found
B7Z3K9	Fructose-bisphosphate aldolase *,†	1(1/4)	1	not found
Q6FH62	HSD17B3	1(1/4)	1	not found
X6R7Y7	Intraflagellar transport protein 25 homolog (HSPB11)	1(1/4)	1	not found
Q96P63-2	Serpin B12 (SERPINB12)	1(1/4)	1	not found
P59665	Neutrophil defensin 1 (DEFA1)	1(1/4)	1	20375.74
P01833	Polymeric immunoglobulin receptor (PIGR) *,†	1(1/4)	1	129844.97
A0A158RFU6	RAB7 †	1(1/4)	1	not found
P29508	Serpin B3 (SERPINB3)	1(1/4)	1	26103.15

Note: * indicates that the protein was identified in the Walker256 model total protein, and † indicates that the protein was identified in the glioma model total protein. The contents after "Identification counts" are expressed as the number of animals/total number of animals in the group.

This shows that in animals with normal immune systems, some differential urinary proteins were closely related to immune response. In immunodeficient animals, differential urinary proteins had little contact with the immune system.

The bioinformatics analysis results for the 42 human proteins are shown in **Figure 3.**

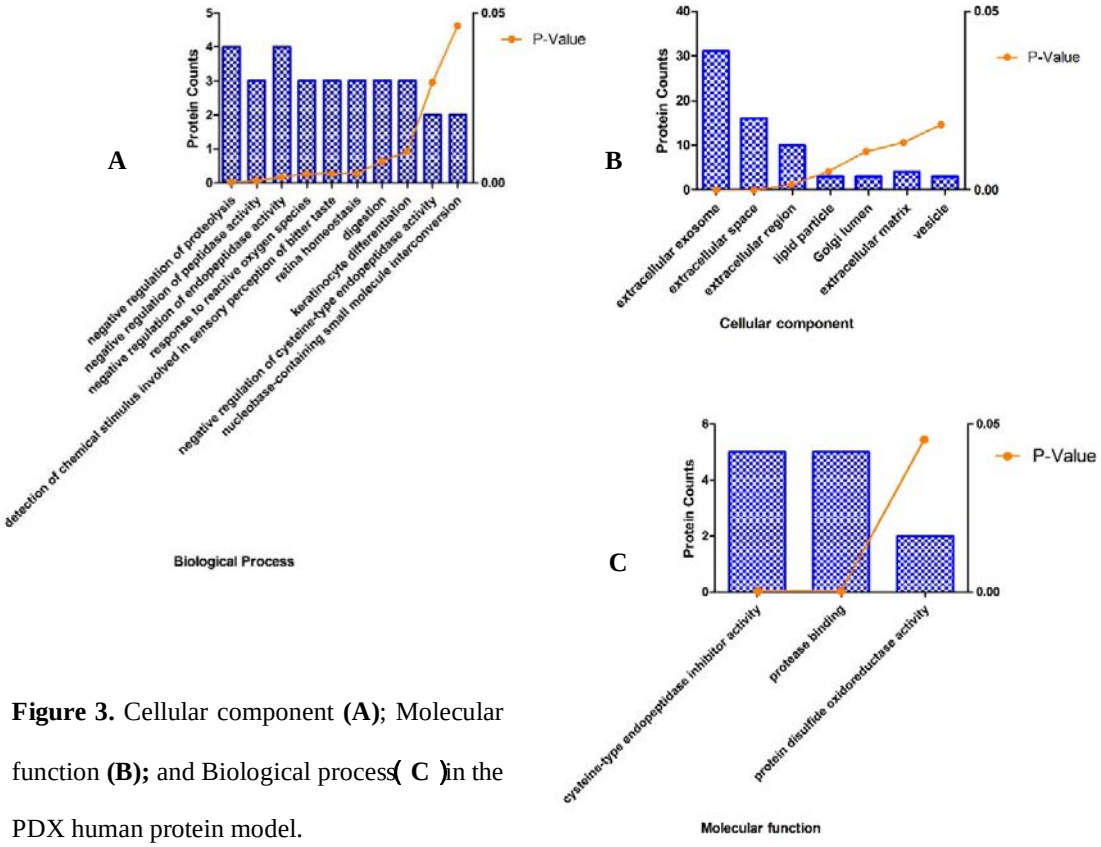

Figure 3. Cellular component **(A)**; Molecular function **(B);** and Biological process **(C)** in the PDX human protein model.

Differential urinary proteins in the host

The methods for screening differential proteins in mouse species are as follows. (1) Each protein contains at least two or more specific peptides. (2) After statistical analysis, the P value of each protein was less than 0.05 with a fold change is greater than 2. (3) The proteins were identified in each sample in the group (4/4), and 8 proteins met the above identification conditions. **Table 2** shows this information in detail.

Table 2. Differential urinary proteins in nude mice

		PDX Model		**Glioma Model**			**Walker 256 tumor-bearing Model**			
Experimental Animals		Nude mouse		Rat			Rat			
Immune System		T cell Immunodeficient		Immunocompetent			Immunocompetent			
Time Node/Day		23	2	6	10	13	4	6	9	14
Differential Proteins		8	56	65	61	27	7	17	92	31
Total Proteins		515		778			533			
Screening Criteria	**Unique Peptide**	> 2								
	Fold Change	> 2								
	P-Values	< 0.05								
	Number in Group	4/4		3/3			4/4			

Accession	Protein description	Discovery	Unique Peptide	Fold Change	P-Values	Trends	Homologous protein

Q5FW60	Major urinary protein 20 (Mup20)	Control group &Tumor group	9	6.25	0.01051	Lower	No
B0V388	Novel member of the major urinary protein (Mup) gene family	Control group &Tumor group	5	5.88	0.02104	Lower	No
A2ARV4	Low-density lipoprotein receptor-related protein 2 (Lrp2)	Control group &Tumor group	77	2.73	0.04849	Up	Yes
P28843	Dipeptidyl peptidase 4 (Dpp4)	Control group &Tumor group	17	2.97	0.03824	Up	Yes
Q03265	ATP synthase subunit alpha, mitochondrial (Atp5a1)	Tumor group	3	-	-	-	Yes
G3XA48	Isopentenyl-diphosphate Delta-isomerase 1 (Idi1)	Tumor group	3	-	-	-	Yes
G3UYJ7	Predicted gene 20441 (Gm20441)	Tumor group	3	-	-	-	No
P52787	Gastric intrinsic factor (Gif)	Control group	5	-	-	-	Yes

The differential protein information obtained from these results was compared with Wu's Walker256 rat model and Ni's glioma rat model at different time nodes (**Table 3**).

Table 3. Comparisons of three tumor models and differential urinary protein information

Urinary protein functional analysis

Biological process analyses were performed on 31 differential proteins on day 14 of the Walker 256 rat model and on 8 differential proteins of the PDX model. The 8 differential proteins of the PDX model were related to only the transport process (protein counts=3, p=0.083).

However, 32 biological processes were found in the Walker 256 rat model, many of which are related to immunity, such as complement activation, positive B-cell activation regulation, innate immune response, phagocytosis, the B-cell receptor signaling pathway, factor XII activation, and the immune system (**Table 4**). Compared with differential urinary proteins from tumor-bearing immuno-competent rats, the differential urinary proteins in the PDX model have none of the host immune response proteins found in the tumor-bearing immuno-competent rat model urine.

Table 4. Biological process analysis on day 14 of the Walker 256 rat model and PDX models

Model	Biological Processes	Count	P-Value
Walker 256 (Only shows biological processes with P-values less than 0.05)	complement activation, classical pathway	5	8.40E-07
	acute-phase response	4	5.90E-05
	defense response to bacterium	5	1.40E-04
	negative regulation of endopeptidase activity	5	2.10E-04
	organ regeneration	4	7.80E-04
	positive regulation of B cell activation	3	8.70E-04
	phagocytosis, recognition	3	1.20E-03
	innate immune response	5	1.70E-03
	phagocytosis, engulfment	3	2.20E-03
	inflammatory response	5	2.80E-03

	negative regulation of tumor necrosis factor production	3	3.50E-03
	response to drug	6	3.70E-03
	B cell receptor signaling pathway	3	3.80E-03
	hemoglobin import	2	4.00E-03
	vitamin metabolic process	2	4.00E-03
	Factor XII activation	2	6.00E-03
	cobalamin transport	2	8.00E-03
	proteolysis	5	1.40E-02
	positive regulation of dendritic cell chemotaxis	2	1.60E-02
	response to lipopolysaccharide	4	1.80E-02
	tissue remodeling	2	2.40E-02
	aging	4	2.50E-02
	carbohydrate metabolic process	3	2.60E-02
	lipoprotein transport	2	2.80E-02
	apoptotic process	4	3.60E-02
	immune system process	2	4.90E-02
PDX (all biological processes)	transport process	3	8.30E-02

Can the human proteins identified in the PDX be present in the urine of immuno-competent animals? Comparing 42 human proteins with the total urinary proteins identified by the Walker 256 and glioma rat models, 10 were identified in both models, 5 were identified in only the glioma rat model, and 1 was identified in only the Walker 256 model. The remaining 26 human proteins were not found in the total proteins of the other two models. This suggests that some human-origin tumor proteins identified in the PDX model may also be present in the urine of immuno-competent animals.

Conclusion

Human-origin tumor proteins can be identified in PDX mouse urine. The differential urinary proteins in the PDX model had none of the host immune response proteins commonly found in the very early urinary stages in the tumor-bearing immuno-competent rat models.

References

[1] Gao YH. Urine-an untapped goldmine for biomarker discovery?[J] China Life Sci, 2013, 56(12): 1145-1146.

[2] WU JQ, GUO ZG, GAO YH. Dynamic changes of urine proteome in a Walker 256 tumor-bearing rat model[J]. Cancer Medicine. 2017,10(04):1-10.

[3] Yanying Ni. Early candidate biomarkers found from urine of astrocytoma rat before changes in MRI[J].BioRxiv.

[4] WU JQ, Li XD, GAO YH et.al. Early detection of urinary proteome biomarkers for effective early treatment of pulmonary fibrosis in a rat model[J]. Proteomics - Clinical Applications.2017,10(04):1-38.

[5] Zhang FS, Ni YY, Yuan Y and Gao YH. Urinary proteome changes were detected earlier than serum biochemical parameters and histopathology changes in a rat thioacetamide-induced hepatic[R]. ASPET. 2017.4.

[6] Gao YH. Patient-Derived Xenograft Models for Urinary Biomarker Discovery[J]. Med Crave. 2016.1(1).

[7] Sun W, Li FX, Wu SZ, et al. Human urine proteome analysis by three separation approaches[J]. Proteomics, 2005, 5(18): 4994-5001.

[8] Zhang Y, Hodgson NW, Trivedi MSD et al.ecreased Brain Levels of Vitamin B12 in Aging, Autism and Schizophrenia[J].PLoS One. 2016, 11(1):1-10.

[9] ZHAO MD, GAO YH, et al.A comprehensive analysis and annotation of human normal urinary proteome[J]. Scientific reports.2017,8(8).

[10] Nandy SK, Seal A. Structural Dynamics Investigation of Human Family 1 & 2 Cystatin-Cathepsin L1 Interaction: A Comparison of Binding Modes[J].PLoS One.2016,11(10):1-18.

[11] Algarni AA, Mussi MC, Moffa EB et al. The impact of stannous, fluoride ions and its combination on enamel pellicle proteome and dental erosion prevention[J].PLoS One.2015,10(6).

[12] Perumal N, Funke S, Wolters D, et al. Characterization of human reflex tear proteome reveals high expression of lacrimal proline-rich protein 4 (PRR4)[J].Proteomics.2015,15(19):70-81.

[13] Fernandez-Olavarria A, Mosquera-Perez R, Diaz-Sanchez RM et al.The role of serum biomarkers in the diagnosis and prognosis of oral cancer: A systematic review[J].J Clin Exp Dent. 2016,8(2):84-93.

[14] Emmink BL1, Verheem A, Van Houdt WJ,et al.The secretome of colon cancer stem cells contains drug-metabolizing enzymes[J].Proteomics, 2013,10(8):84-96.

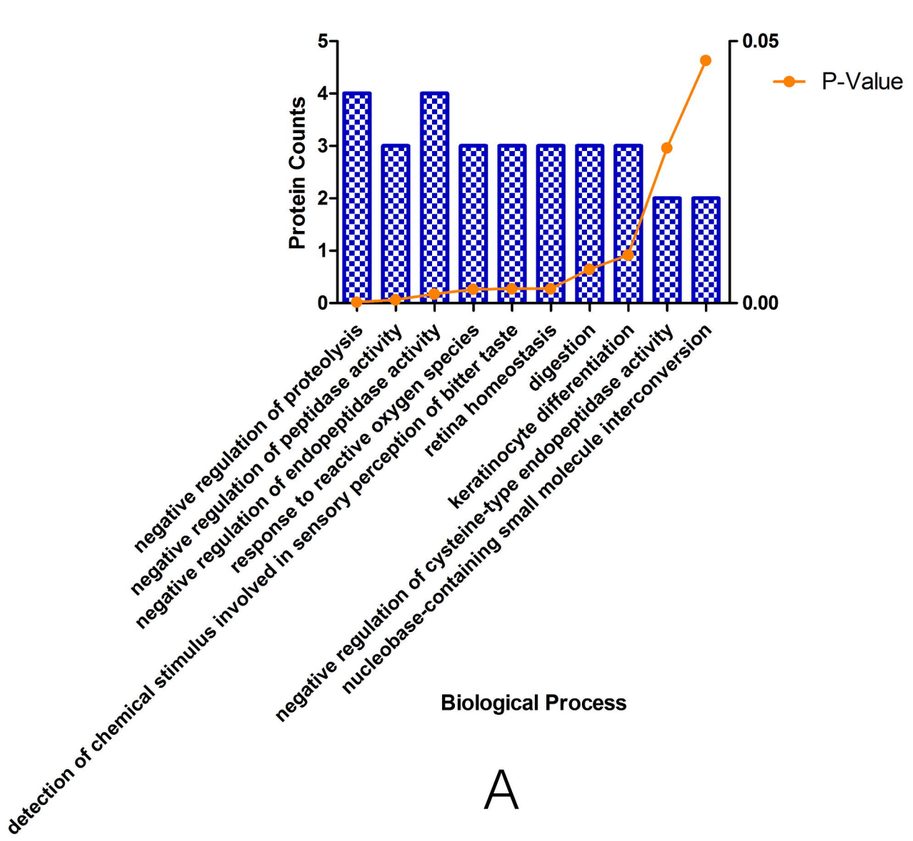
Protein Counts
P-Value
0.05
0.00
negative regulation of proteolysis
negative regulation of peptidase activity
negative regulation of endopeptidase activity
response to reactive oxygen species
detection of chemical stimulus involved in sensory perception of bitter taste
retina homeostasis
digestion
keratinocyte differentiation
negative regulation of cysteine-type endopeptidase activity
nucleobase-containing small molecule interconversion
Biological Process

A

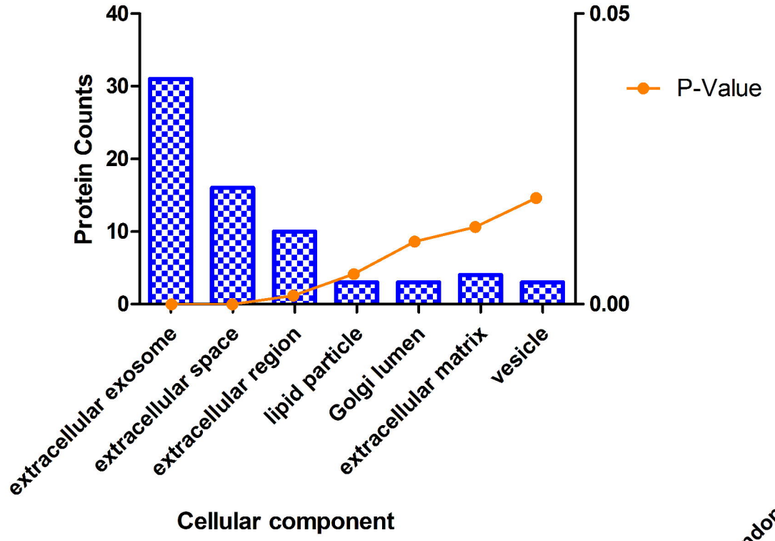
Protein Counts
P-Value
0.05
0.00
extracellular exosome
extracellular space
extracellular region
lipid particle
Golgi lumen
extracellular matrix
vesicle
Cellular component

B

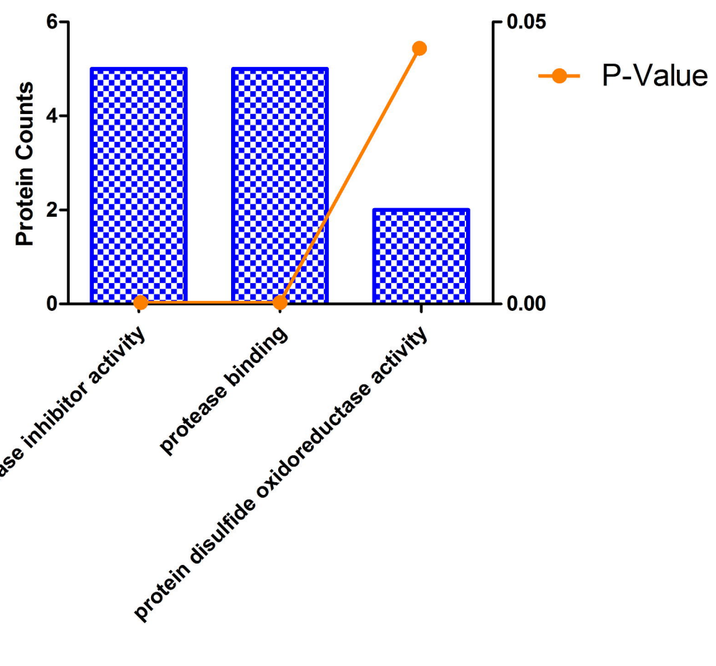
Protein Counts
P-Value
0.05
0.00
cysteine-type endopeptidase inhibitor activity
protease binding
protein disulfide oxidoreductase activity
Molecular function

C

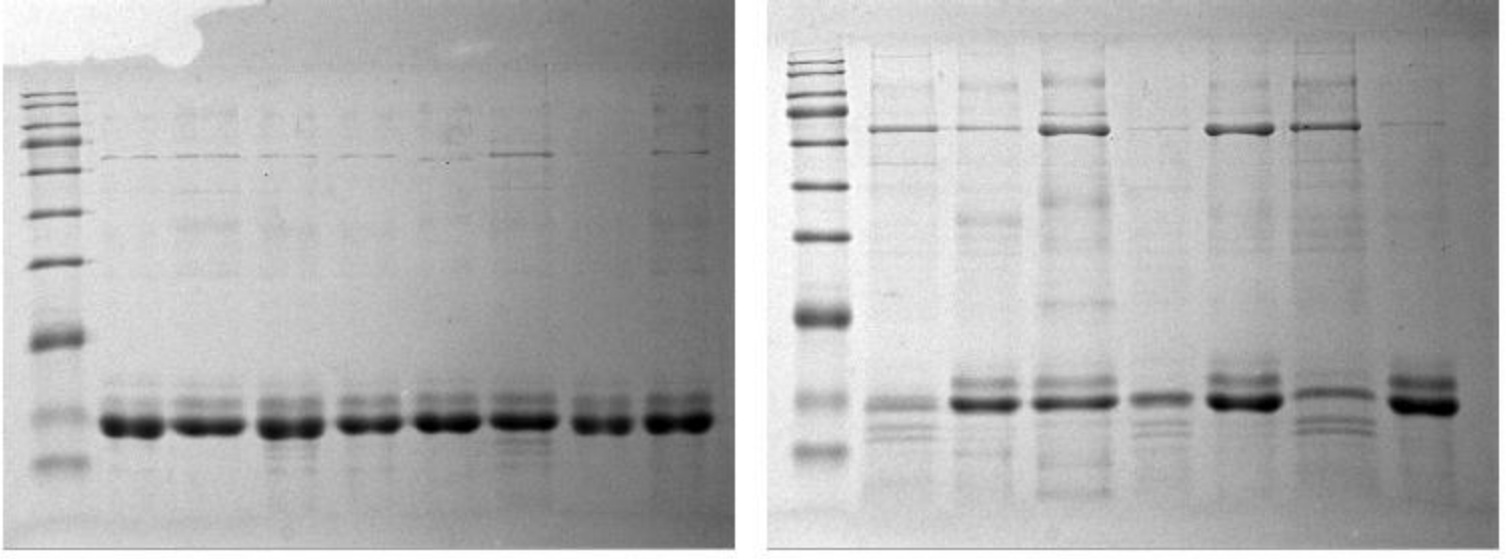

A

B